

Using Gravitational Wave Parallax to Measure the Hubble Parameter with Pulsar Timing Arrays

Daniel J. D’Orazio* and Abraham Loeb

Department of Astronomy, Harvard University, 60 Garden Street Cambridge, MA 02138, USA

We demonstrate how pulsar timing arrays (PTAs) yield a purely gravitational wave (GW) measurement of the luminosity distance and co-moving distance to a supermassive black hole binary source, hence providing an estimate of the source redshift and the Hubble constant. The luminosity distance is derived through standard measurement of the chirp mass, which for the slowly evolving binary sources in the PTA band can be found by comparing the frequency of GW-timing residuals at the Earth compared to those at distant pulsars in the array. The co-moving distance can be measured from GW-timing parallax caused by the curvature of the GW wavefronts. This can be detected for single sources at the high-frequency end of the PTA band out to 10 Gpc with a future PTA containing well-timed pulsars out to $\mathcal{O}(10)$ kpc. We estimate that for a future PTA with $\mathcal{O}(100)$ pulsars between 1 and 20 kpc and $\sim 1\%$ pulsar-distance errors, the Hubble constant can be measured to better than 30% for a single source at $0.1 \lesssim z \lesssim 2$. At $z \lesssim 0.1$, the luminosity and co-moving distances are too similar to disentangle. At $z \gtrsim 2$, this measurement will be restricted by a signal-to-noise ratio threshold.

I. INTRODUCTION

Gravitational waves (GWs) from coalescing compact object binaries are now being used to measure cosmological parameters. This new handle on cosmology is an important tool for understanding systematics in our current measurements of the cosmological parameters, *e.g.*, for resolving the existing tension between different measures of the Hubble constant [1–3].

Direct measurements of the Hubble constant rely on knowledge of the redshift of an emitting source in addition to a determination of its intrinsic luminosity, be it GW or electromagnetic (EM), which is used to determine the luminosity distance. Comparison of the redshift and distance yields the Hubble constant. For example, the backbone of the standard candle approach [2] leverages the Leavitt Law [4] to relate the oscillation period of Cepheid variable light-curves to the intrinsic luminosity, while a redshift is measured from the frequency shift of spectral lines in the host galaxy. The standard sirens approach [5–10] uses the predicted GW strain and frequency evolution of a coalescing binary to determine a luminosity distance, while again relying on an EM determination of the redshift, z .

While both are vital techniques, contributing independent measures of cosmology, the former relies on theoretical knowledge of standard candles and their astrophysical environments, *e.g.*, supernovae, [11] while the latter relies on the existence of an EM counterpart that can be identified with the GW source, and hence understanding EM emission mechanisms. Additionally, both approaches only apply out to distances where EM emission can be detected.

The few methods that have been proposed to make cosmological measurements with GWs alone make use of inferred knowledge of the rest-frame GW source properties. For example, [12, 13] rely on models of the rest frame neutron star mass distribution to break the mass-redshift degeneracy of inspiraling neutron star binaries. This is required because of the scale invariance of the binary merger problem. The GW luminosity is independent of the binary mass, and the quan-

tity $\mathcal{M}f$, the so called chirp mass times the GW frequency, is invariant with redshift. Hence, one must obtain knowledge about intrinsic source properties to make a joint redshift and luminosity distance determination, or one must introduce a new scale to the problem.

Here we do the latter. We propose a method for probing the distance-redshift relationship, and hence, measure the Hubble constant, via gravity alone, and without making assumptions about the GW source. While we cannot break the scale invariance of the binary merger problem, we can infer the redshift through a different means, with a large detector whose components are separated widely enough to detect the GW wavefront curvature. Measurement of this curvature through timing parallax will provide a distance to the source that is formally a co-moving distance. The co-moving distance, D_c , is related to the luminosity distance, D_L , through $D_c = (1+z)^{-1}D_L$. A separate determination of the luminosity distance from the GW chirp and amplitude gives the redshift. Comparison of redshift and luminosity distance yields the Hubble constant up to choices of the cosmological density parameters.

Such a determination of the co-moving distance from GW wavefront curvature is not possible with current interferometric GW detectors such as LIGO [14] and LISA [15], which are sensitive to GWs from compact-object binary mergers ranging in mass from a few to $\sim 10^7 M_\odot$. However, Ref. [16] (hereafter DF11) shows that it is possible with the galaxy-scale Pulsar Timing Arrays [PTAs, 17], which are expected to detect low frequency GWs from the biggest black hole mergers in the universe with masses of $10^8 - 10^{10} M_\odot$, within the next decade [18]. We re-derive this result with the important clarification that the distance recovered in this manner is indeed a co-moving distance, not a luminosity distance as posited in DF11.

II. DISTANCE MEASUREMENTS WITH PTAS

The PTAs employ millisecond pulsars (MSPs) across the galaxy as precise clocks. A GW passing through the Earth-pulsar array will cause detectable deviations in the arrival times of the otherwise steady pulses that, when meticulously separated from non-GW induced timing residuals due to the

* djdorazio@gmail.com

intervening Earth-pulsar medium [19], will allow detection of GWs in the 1-100 nHz frequency band. This is the relevant band for tracking the late inspiral of the most massive, $10^8 - 10^{10} M_\odot$ black holes binaries at the hearts of massive galaxies [20].

Unlike their high-frequency interferometric-detector cousins, LIGO and LISA, one of the PTA's primary targets is a stochastic background of GWs, an astrophysical noise floor generated by the superposition of many inspiraling massive black hole binaries across cosmic distance [21, 22]. Above this noise floor, it is expected that a number of single resolved binary sources will also be detected, where different population models place this number at $\mathcal{O}(1-10)$ for near future arrays [18, 23–25]. Here, we focus on the single resolved binary sources and show how a luminosity distance and a co-moving distance can be measured for a subset of them.

A. Luminosity Distance

It is well known that the luminosity distance can be measured for binary GW sources when their frequency evolution can be detected [e.g., 5, 9]. So called chirping binaries allow measurement of the chirp mass \mathcal{M} and the GW strain h . In the source frame these are related by

$$h \propto \frac{\mathcal{M}_s^{5/3} f_s^{2/3}}{D_c}, \quad (1)$$

where r denotes the source frame and D_c is the co-moving distance. Because the strain h and GW frequency f can be measured over time, and the chirp mass can be measured from the first time derivative of the frequency [or the chirp, see 7, 26], Eq. (1) allows a measurement of the distance. In the observer's frame, the redshift of the frequency and its derivative implies that the strain, written in terms of observables, reads

$$h \propto \frac{\mathcal{M}_o^{5/3} f_o^{2/3}}{D_L}, \quad (2)$$

where o denotes the observer's frame and the measurable distance is $D_L = (1+z)D_c$, the luminosity distance.

Whether or not a binary is chirping in the detectable band is set by the timescale for GW frequency evolution. For a binary on a circular orbit,

$$t_{\text{chirp}} \sim \frac{f}{\dot{f}} = \frac{5}{96} \left(\frac{GM}{c^3} \right)^{-5/3} (\pi f)^{-8/3} \quad (3)$$

$$\approx 5.43 \times 10^3 \text{yr} \left(\frac{\mathcal{M}}{10^9 M_\odot} \right)^{-5/3} \left(\frac{f}{\text{yr}^{-1}} \right)^{-8/3}.$$

For the high frequency and low mass binary inspirals and mergers detected by LIGO ($M = 1 - 10^3 M_\odot$, $f = 10 - 10^4$ Hz), and in the future, by LISA ($M = 10^2 - 10^7 M_\odot$, $f = 10^{-4} - 10^{-1}$ Hz), t_{chirp} is short compared to observation times and determination of the chirp mass and luminosity distance is expected. For the PTAs, however, Eq. (3) shows

that the time for the GW frequency to evolve in the PTA band can be thousands of years. Hence, it is usually assumed that only the combination $\mathcal{M}_o^{5/3}/D_L$ is measurable for binary GW sources in the PTA band.

However, a number of works discussed below have pointed out that chirp information in the PTA band can be gleaned by incorporating the many thousand year light travel time across the Earth-pulsar detector. Because the timing residuals measured on Earth are a culmination of the entire path traveled by a EM pulse between the pulsar and Earth, the chirp can be detected by comparing the GW signal at the pulsar (pulsar term) compared to the signal at Earth (Earth term). Chirp detection then requires that the change in GW frequency at the detector (Earth-pulsar system), over the course of the light travel time across the detector, be larger than the frequency resolution of the detector. Conservatively, the frequency resolution is given by the inverse of the observation time, $\Delta f = 1/t_{\text{obs}}$ [e.g., 27, 28]. Hence the condition on the Earth-pulsar distance L needed to measure the GW chirp is,

$$L \geq \frac{c}{\dot{f} t_{\text{obs}}} \approx 0.08 \text{kpc} \left(\frac{\mathcal{M}}{10^9 M_\odot} \right)^{-5/3} \left(\frac{f}{\text{yr}^{-1}} \right)^{-8/3} \left(\frac{t_{\text{obs}}}{20 \text{yr}} \right)^{-1}. \quad (4)$$

For standard pulsar distances in present day PTAs of 0.1 – 1 kpc, this condition is met for the high frequency, high mass end of the expected SBHB binary population detectable by the PTAs. Longer pulsar baselines of future arrays, reaching out to 20 kpc (see §III A), could allow chirp detection from the largest, $10^{10} M_\odot$, binaries down to a few 10^7 's of nHz, or from the smaller, $10^8 M_\odot$, binaries at ~ 100 nHz.

The parameter space of binaries that meet this criterion and have a detectable strain is explored further in Ref. [29], while Ref. [30] discusses the region of binary parameter space where assuming zero-frequency evolution could be detrimental for detection. Ref. [27] uses the synthetic population of SBHBs from Ref. [23] and shows that the majority will have resolvable chirps when taking into account the pulsar term. While both studies point this out, the primary focus of these works is not binary frequency evolution, and so the chirp was ignored. Ref. [31], however, investigates recovery of the luminosity distance with PTAs from such pulsar-term, chirping binaries. They assume an SNR = 20 detection, with 20 pulsars each having a 100 ns timing residual and randomly oriented on the sky at distances between 0.5 – 1 kpc. They find that the fractional error on the distance can be as low as 7% for edge-on inclination binaries ($i = \pi/2$) and rises to 30% for $i = \pi/4$. We take the findings from the above studies as conservative estimates of how well the luminosity distance can be recovered as they each assume pulsar distances on the order of 1 kpc, where, as motivated in the next section, we are interested in near-future PTAs that could contain well-timed pulsars out to 20 kpc.

B. Co-moving Distance

We now show for the first time how PTA observations of GWs from a resolved, single-binary source can independently

measure the source *co-moving distance*.

1. Geometrical Argument

The amount by which the arrival time of the EM pulses to Earth deviates due to a passing GW is dependent upon the changing amplitude, frequency and phase of the GW encountered by the EM pulse as it traverses the Earth-pulsar distance. This is dependent on the shape of GW wavefronts, surfaces of constant GW phase, across the Earth-pulsar system. For very distant GW sources, the GW wavefronts can be assumed to be planar. However, for nearby sources, the true spherical nature of the wavefronts becomes non-negligible and encodes the source distance.

Panel a) of Figure 1 illustrates a geometrical argument that elucidates this concept and provides an estimate of when wavefront curvature is important. Our setup consists of the detector: Earth and a pulsar separated by a distance L aligned at an angle θ relative to the line of sight of a source of GWs with observed frequency f at co-moving distance D_c .

Without loss of generality, we consider the case where, under the plane wave approximation, GWs emitted at some time in the source frame arrive at the Earth and the pulsar after the same travel time. For spherical wavefronts, the travel time to the pulsar differs by $\delta t = \delta x/c$ (panel a) in Figure 1), causing an EM pulse to experience a different portion of the GW phase. In co-moving (flat-space) coordinates, we can compute δt via Euclidean geometry,

$$\delta t = \frac{D_c}{c} \left[\sqrt{1 + \left(\frac{L}{D_c}\right)^2} - 1 \right] \approx \frac{1}{2} \left(\frac{L}{D_c}\right) \frac{L}{c}. \quad (5)$$

This extra travel time compared to the plane wave case only affects the pulse arrival time if the EM pulse encounters a significant extra portion of a GW cycle. Hence, a condition on there being a significant difference between timing residuals in the plane-wave and spherical-wave cases is found from requiring that $\delta t f \gtrsim 1$ (noting that at exact integer values there is no change). This places a limit on the distances D_c and L for which wavefront curvature is important,

$$D_c \lesssim f \frac{L^2}{c} = \left(\frac{L}{\lambda}\right) L, \quad (6)$$

where $\lambda = f/c$, in analogy to the Fresnel condition in optics.

Because our observable is influenced by the relative time of arrival of GW wavefronts across the Earth-pulsar system, the distance to the source, D_c , must be a co-moving distance that takes into account time dilation along the path of GWs from the source at an earlier time in the universe,

$$D_c = c \int_{t_{\text{src}}}^{t_0} \frac{dt}{a(t)}, \quad (7)$$

where $a(t)$ is the scale factor of the expanding universe at time t , t_0 denotes the observation time, and t_{src} denotes the emission time at the source. Because f and L are present-day

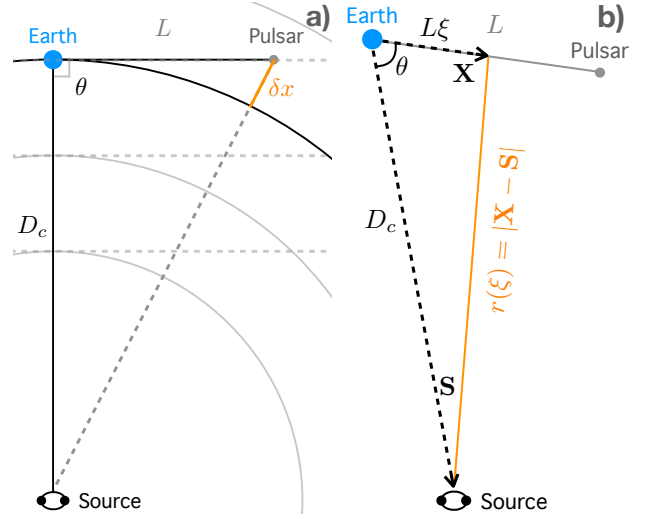


FIG. 1. Schematics for visualizing the geometrical (panel a), §II B 1) and mathematical (panel b), §II B 2) description of the co-moving distance measurement. In panel a), we assume $\theta = 90^\circ$ to simplify the geometrical argument.

observed quantities in Eq. (6), it is the *co-moving* distance that is encoded in the pulsar timing residuals measured at Earth. Another way to see this is to recognize that the GW phase, Φ , is the relevant quantity governing the timing residual, and the GW phase, $\Phi \propto \int f(1+z)dt$, where $f(1+z)$ is the GW frequency at redshift z along the path. Since $a(t) = (1+z)^{-1}$, then $\Phi \propto \int \frac{dt}{a(t)} \propto D_c$.

2. Mathematical Argument

Following DF11, we outline the derivation of the timing residual correction due to curved GW wavefronts. Building upon our previous setup, we illustrate relevant quantities for the derivation in panel b) of Figure 1

Assuming that the pulsar emits regular pulses at a much higher frequency than that of the passing GW [however, see 32], the extra light travel time of a given pulse due to the passing GW, the arrival time correction, is given by [33–35],

$$t_{\text{GW}}(t) = -\frac{1}{2} \hat{n}^i \hat{n}^j \mathcal{H}_{ij} \quad (8)$$

$$\mathcal{H}_{ij} = \frac{L}{c} \int_{-1}^0 h_{ij} \left[t + \frac{L}{c} \xi, -L \xi \hat{n} \right] d\xi, \quad (9)$$

which is the integral of each component of the transverse-traceless GW metric perturbation $h_{ij}(t, \mathbf{x})$ along a null geodesic connecting the pulsar and the Earth, parameterized by ξ . Here \mathbf{P} is the position of the pulsar and \hat{n} is the unit vector pointing from Earth to the pulsar.

Writing out the strain as a function of the spacetime coordinates in the source frame, and in terms of the Fourier com-

ponents,

$$h_{ij}(t, \mathbf{X}) = \frac{1}{|\mathbf{X} - \mathbf{S}|} \int_{-\infty}^{\infty} \left[\tilde{A}_{ij}(f_s, \hat{\mathbf{k}}) e^{2\pi i f_s |\mathbf{X} - \mathbf{S}|/c} \right] e^{-2\pi i f_s t} df_s d^3 k. \quad (10)$$

where the s subscript labels the source frame with no red-shifting of the frequency. Here \mathbf{X} is the vector pointing from Earth to the EM pulse wavefront that is traveling the null geodesic connecting the Earth and pulsar, $\mathbf{X} = L\xi\hat{\mathbf{n}}$. \mathbf{S} is the vector pointing from the Earth to the source, $\mathbf{S} = D_c\hat{\mathbf{s}}$, where D_c is the co-moving distance to the source. The quantities \tilde{A}_{ij} are the components of the wave strength.

The spherical GW wavefront propagates along the unit vector,

$$\hat{\mathbf{k}} = \frac{\mathbf{X} - \mathbf{S}}{|\mathbf{X} - \mathbf{S}|}. \quad (11)$$

The magnitude $|\mathbf{X} - \mathbf{S}|$, namely the distance from source to wavefront at point $\mathbf{X}(\xi)$, can be found by the law of cosines. For a flat universe in co-moving coordinates,

$$r(\xi) \equiv |\mathbf{X} - \mathbf{S}| = D_c \left[1 + \left(\frac{L\xi}{D_c} \right)^2 + 2 \frac{L\xi}{D_c} \cos \theta \right]^{1/2}. \quad (12)$$

Note that the GW amplitude is proportional to $\tilde{A}_{ij}/r(\xi)$, which reduces to \tilde{A}_{ij}/D_c , as expected for $D_c \gg L$.

Combining Eqs. (8-12), keeping terms to $\mathcal{O}(L/D_c)$, integrating, and separating terms in order of L/D_c , we find the expression for the plane-wave and first-order-curvature GW-timing residuals, matching Eq. (10) of DF11. To write their

$$\begin{aligned} \tau_{\mathcal{GW}} = \tau_{\text{pw}} + \tau_{\text{cr}} = \frac{\Delta T_o}{2} \left\{ \exp \left(2\pi i f_o L \sin^2 \frac{\theta}{2} \right) \frac{\sin \left(2\pi f_o L \sin^2 \frac{\theta}{2} \right)}{\sin^2 \frac{\theta}{2}} + \right. \\ \left. + 2(1 + \cos \theta) \exp \left[\pi f_o L \left(4 \sin^2 \frac{\theta}{2} + \frac{L}{2D_c} \sin^2 \theta \right) \right] \frac{\sin \left(\frac{\pi f_o L^2}{2D_c} \sin^2 \theta \right)}{\sin^2 \theta} \right\}. \quad (16) \end{aligned}$$

Both terms still have a dependence on the distance through the usual $1/D_L$ in ΔT_o . However, the curvature term now has a dependence on $f_o L^2/D_c$. *Because we can independently measure f_o and L , this term introduces a way to measure the co-moving distance separately from the luminosity distance.*

The form of the residual also confirms our simple geometric argument of the previous subsection, that the curvature term decreases in importance as $\pi f_o L^2/D_c \sin^2 \theta \rightarrow 0$. Indeed when $D_c \gg \frac{f_o L^2}{c}$, the wavefront curvature can be neglected. For values typical of contemporary and near future PTAs,

$$\frac{\pi f_o L^2}{D_c} = 0.1 \left(\frac{f_o}{\text{yr}^{-1}} \right) \left(\frac{L}{1 \text{ kpc}} \right)^2 \left(\frac{D_c}{100 \text{ Mpc}} \right)^{-1}. \quad (17)$$

However, the dependence on pulsar distance is quadratic.

expression in a more elucidating form, we define

$$\begin{aligned} \Delta T \equiv \frac{[\hat{n}^i \hat{n}^j \tilde{A}_{ij}]_s}{2\pi f_o D_c} e^{2\pi i f_s D_c/c} \\ \propto \frac{\mathcal{M}_s^{5/3} f_s^{2/3}}{2\pi f_o D_c} e^{2\pi i f_s D_c/c} \mathcal{Q}(\alpha_P, \beta_P, \phi, \phi_0, I, \psi) \quad (13) \end{aligned}$$

where in the last line we write out the \tilde{A}_{ij} dependence assuming circular binary orbits. The function \mathcal{Q} depends on the pulsar position angles (α_P, β_P) , the binary orbital phase ϕ and phase reference ϕ_0 , the binary inclination I , and the polarization angle ψ . The other two angles of importance, the angular position of the GW source (α, β) , appear outside of ΔT through the angle θ ,

$$\cos \theta = \cos \beta \cos \beta_P \cos(\alpha - \alpha_P) + \sin \beta \sin \beta_P. \quad (14)$$

Importantly, the denominator of Eq. (13) includes the frequency at the Earth-pulsar detector. This is because the observed timing residual is set by the observed strain over the observed GW frequency. To put the above into observed quantities for sources at cosmological distance, use that $\mathcal{M}_o = (1+z)\mathcal{M}_s$ and $f_o = (1+z)^{-1}f_s$. Therefore,

$$\frac{\Delta T_o}{\mathcal{Q}(\alpha_P, \beta_P, \phi, \phi_0, I, \psi)} \propto \frac{\mathcal{M}_o^{5/3} f_o^{-1/3}}{2\pi D_L} e^{2\pi i f_o D_L/c}, \quad (15)$$

where the luminosity distance $D_L = (1+z)D_c$.

Using our definition of ΔT_o , the timing residual, broken into plane-wave and first-order curvature parts, becomes

Hence, if future PTAs can precisely time pulsars out to 10 kpc, then the co-moving distance can be probed through GW timing parallax out to 10 Gpc, or $z = 12$, for all conceivable SBHB mergers detectable by PTAs.

III. HUBBLE CONSTANT MEASUREMENT

When both the luminosity distance and the co-moving distance can be measured, and distinguished from each other, for the same binary GW source, the redshift and hence Hubble constant H_0 can be measured. To distinguish the two distances we require that the fractional errors on D_L and D_c be less than $(D_L - D_c)/D_c = z$, which is ~ 0.25 at 1 Gpc.

When this is possible, the redshift of the source can be recovered with uncertainty,

$$\delta z = \sqrt{\left(\frac{\delta D_L}{D_c}\right)^2 + \left(\frac{D_L}{D_c} \frac{\delta D_c}{D_c}\right)^2} \quad (18)$$

and can be used to measure the Hubble constant via,

$$H_0 = \frac{c}{D_c(z)} \int_0^z \frac{dz'}{E(z')}, \quad (19)$$

with relative uncertainty,

$$\frac{\delta H_0}{H_0} = \sqrt{\left(\frac{\delta z}{E(z)}\right)^2 \left(\int_0^z \frac{dz'}{E(z')}\right)^{-2} + \left(\frac{\delta D_c}{D_c}\right)^2}. \quad (20)$$

A. Distance Measurement Precision and PTA Dependence

We estimate the fractional error in the Hubble constant measurement by considering PTA detections only above a cutoff SNR and hence a constant fractional error on D_L . As a fiducial value we use $\delta D_L/L \sim 10\%$ estimated in [31] for detections with a signal-noise-ratio (SNR) of 20 (see §II A). Next, we numerically estimate the precision in the $D_c(z)$ measurement.

As we aim at a proof-of-principle calculation, we provide only an idealized treatment focusing on the recovery of the source co-moving distance and angular coordinates. As pointed out in DF11, the most stringent requirement is precise knowledge of the pulsar distances. Hence, our error analysis focuses on the pulsar distance error and an approximate GW-timing-residual error discussed below.

We envision an idealized PTA with N_p pulsars having randomly drawn angular coordinates (α_i, β_i) on the sky, at randomly drawn distances L_i in the range L_{\min} to L_{\max} , and with constant fractional distance errors $\delta L/L$. We consider further that, for each pulsar, the timing residual divided by the prefactor ΔT_o in Eq. (16) can be measured to within a constant fractional error of $\delta\tau/\tau$. This essentially subsumes errors on the remaining binary parameters into $\delta\tau_i$ and will generally be dependent on the SNR.

We generate mock observed timing residuals by calculating the expected timing residual, τ_i , from Eq. (16). We draw ‘observed’ values $\tau_{\text{obs},i}$ from a normal distribution with mean and standard deviation given by τ_i and $\delta\tau_i$, respectively. We also draw ‘observed’ pulsar distances $L_{\text{obs},i}$ from a normal distribution with mean and standard deviation given by L_i and δL_i , respectively. We recover the source parameters from the observed timing residuals by comparing to the model, Eq. (16), but with $L_{\text{obs},i}$ as the input pulsar distances. To do so, we sample the 3-D posterior probability distribution of source parameters using the affine invariant Markov-Chain Monte Carlo (MCMC) implementation, `emcee` [36, 37]. We adopt a least square’s statistic,

$$\sum_{i=1}^{i=N_p} (\tau_{\mathcal{GW}}(D_c, \alpha, \beta, L_{\text{obs},i}) - \tau_{\text{obs},i})^2, \quad (21)$$

as a likelihood function, and impose a log-uniform prior on $\log D_c/\text{Mpc} \in [0, 5]$ and uniform priors on the angular source coordinates $\alpha \in [0, 2\pi]$, $\beta \in [0, \pi]$. While the mock-observed $\tau_{\text{obs},i}$ are fixed, we draw a new set of $L_{\text{obs},i}$ for each computation of the likelihood, effectively sampling the error range. We then use the [16%, 50%, 84%] quantile values of the 1D marginalized distributions for each parameter as estimators for the mean and standard deviation of the recovered source parameters.

Throughout we consider a fiducial PTA with N_p pulsars in the $L_{\min} = 1$ kpc, to $L_{\max} = 20$ kpc distance range and a fiducial fractional error on L of 1%. The pulsar distances are motivated by [38] which estimate that the Square Kilometer Array [SKA, 39, 40] will find ~ 9000 pulsars to which distances can be determined to better than 20%. Additionally, [29] show that an SKA-era PTA can measure pulsar distances at 1 kpc to sub-parsec precision, resulting in sub-percent level fractional errors; we extrapolate this to 1% errors at ~ 10 kpc. The fractional error on τ will be SNR dependent; for the purpose of this study, we choose a fiducial value of 10%. We study the affect of varying these choices below.

For computational purposes, we draw pulsar sky locations within $\pi/4$ from the optimal $\theta = \pi/2$. This means that an isotropic pulsar distribution would require twice the number quoted here, though, for a favorably positioned source, a pulsar distribution biased by the Milky Way plane would require less pulsars than our N_p suggests. We find below that a factor of a few in our predicted pulsar numbers is not significant compared to other uncertainties and may not be a limiting issue given that 100’s to 1000’s of pulsars may make up future PTAs [38]. Finally, we consider GW source frequencies between $f_o = 10^{-6.5}$ Hz and $f_o = 10^{-7.5}$ Hz, where the GW parallax distance determination is most effective.

Figure 2 shows how well our fiducial PTA recovers the co-moving distance (left) longitude (middle), and latitude (right) of a $f = 10^{-7}$ Hz GW source when it is placed at a redshift of $z = 0.25$ with angular positions $(\alpha, \beta) = (\pi/4, \pi/4)$. In the top row we vary the number of pulsars in the array. In the bottom row, we vary the fractional error on pulsar distances. We find that the source coordinates are poorly constrained for $N_p \leq 16$. The large offset in accuracy for these small-number arrays is partly due to the bimodal nature of the likelihood function, for few pulsars, the MCMC walkers cannot decide between two peaks located 180° apart on the sky.

For the 32 pulsar array considered in the top row of Figure 2, the co-moving distance is recovered to within 10% at 1 Gpc, while the angular coordinates are recovered to within $\sim 4.5^\circ$. These numbers reach a precision of 4% on the distance and 1.3° on the angular positions for the most optimistic 256 pulsar array.

The 128 pulsar array is studied further in the bottom row of Figure 2, where we vary $\delta L/L$. Here we find that while 10 – 20% fractional error on D_c could be achieved with 10% fractional errors on the pulsar distances, errors are greatly improved to the few percent level when $\delta L/L$ reaches 1%. Recovery of the angular source position is not very sensitive to the pulsar distance measurement for $\delta L/L \leq 0.1$. Hence below we consider PTAs with $N_p \geq 32$ and $\delta L/L = 0.01$.

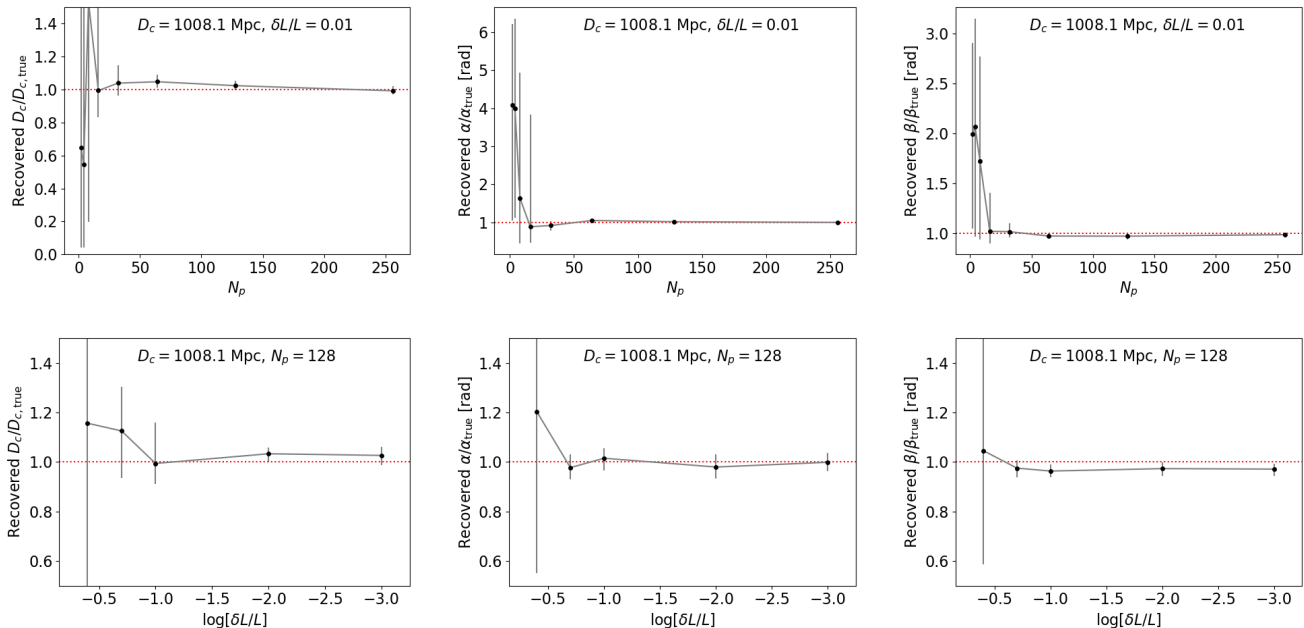


FIG. 2. The recovered co-moving distance, D_c , and sky coordinates, (α, β) , of the GW source for PTAs with varying numbers of pulsars and precision in the distance measurement of these pulsars. The considered PTA assumes pulsars lying between 1 and 20 kpc from Earth and with $\delta\tau/\tau = 0.1$.

B. Precision of Redshift and Hubble Constant Measurement

In the left panel of Figure 3, we plot recovered co-moving distances as a function of redshift (orange) for fiducial PTA and source properties and using 64 pulsars. For reference, we also plot the corresponding luminosity distances with 10% errors (blue). The dotted lines show the theoretical expectation for each distance measure¹. Accurate determination of luminosity and co-moving distances, and hence determination of the source redshift, is possible when recovered values are consistent with the theoretical values, and when the blue and orange error-bars do not overlap.

The right panel of Figure 3 uses the distance errors in the left panel and Eqs. (18) and (20) to display the fractional error in the redshift and the Hubble constant measurements for the corresponding points in the left panel. For this specific GW source ($\alpha = \beta = \pi/4$, $f = 10^{-7}$ Hz) and PTA, we find that the redshift and Hubble constant can be determined to better than order unity for $z \gtrsim 0.1$ and to within 30% for $z \gtrsim 0.5$. At $z \leq 0.1$, D_c and D_L are indistinguishable from each-other, but their measurement could still impose upper limits on z and H_0 .

Figure 4 replicates Figure 3 for less optimistic fractional errors in the pulsar distances, $\delta L/L = 0.2$, but trading off for many more pulsars. Here $N_p = 1024$ assumes that 1 in 9 pulsars with SKA distance measurements [38] could be incorporated into the PTA. In this case, measurements of z and H_0

with better than order unity precision can be made for $z \geq 0.3$, and better than 30% for $z \gtrsim 1$.

Figure 5 replicates Figure 3 but now for an optimistic scenario where 1024 pulsars can be incorporated into a GW PTA with 1% pulsar distance and timing precision, and for a high frequency GW source of $10^{-6.5}$ Hz. In this optimal scenario, the minimum redshift required for order-unity-precision distance measurements remains at $z = 0.1$, but 10% level measurements of the Hubble constant are possible for $z \geq 2$. We do not consider higher redshifts as such binary GW sources are likely not detectable beyond this range with SKA-era PTAs [23].

IV. DISCUSSION AND CONCLUSIONS

We have demonstrated that plausible realizations of PTAs, which are set to detect GWs from SBHBs in the coming decades, will be able to measure both the luminosity distance and the co-moving distance to a subset of these GW sources and in doing so measure the source redshift and the Hubble constant. Thus the PTAs, by themselves, can become cosmological instruments.

Currently, PTAs are operating with tens of pulsars at distances out to a few kpc. Distance errors range from a fraction of a percent to order unity [e.g., 41, 42]. However, in the coming years, the SKA is expected to expand the pulsar population drastically [40]. Ref. [38] estimates that ~ 9000 pulsars are detectable by the SKA out to $\mathcal{O}(10)$ kpc with better than 20% error on their distances. If 1 – 10% of these are suitable for high precision timing, then the PTAs envi-

¹ We use $\Omega_M = 0.3$, $\Omega + \Lambda = 0.7$, and $h = 0.7$ throughout.

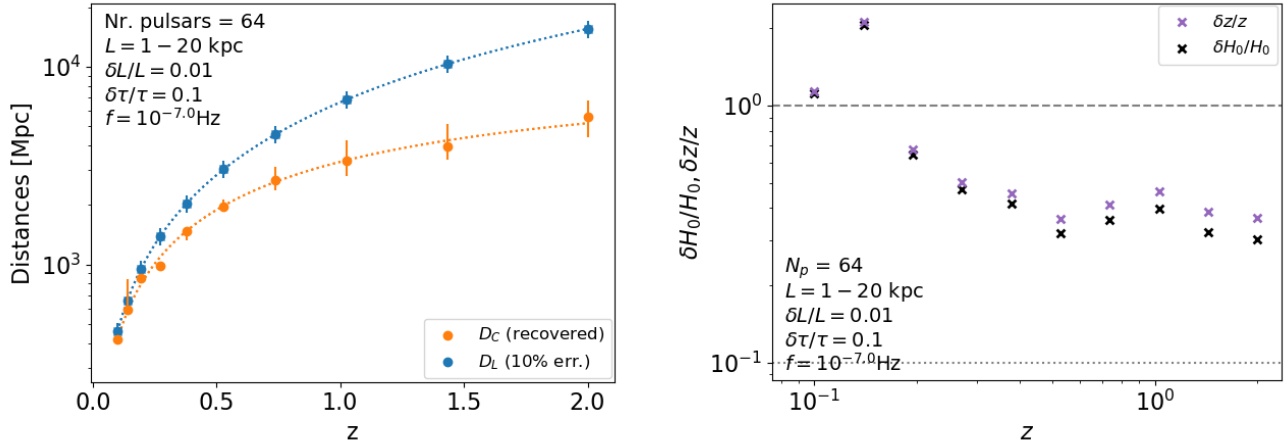


FIG. 3. *Left*: Recovery of co-moving and luminosity distances, D_C and D_L , vs. redshift, z , for an SKA-era PTA. *Right*: the corresponding fractional errors in the measured redshift and the Hubble constant.

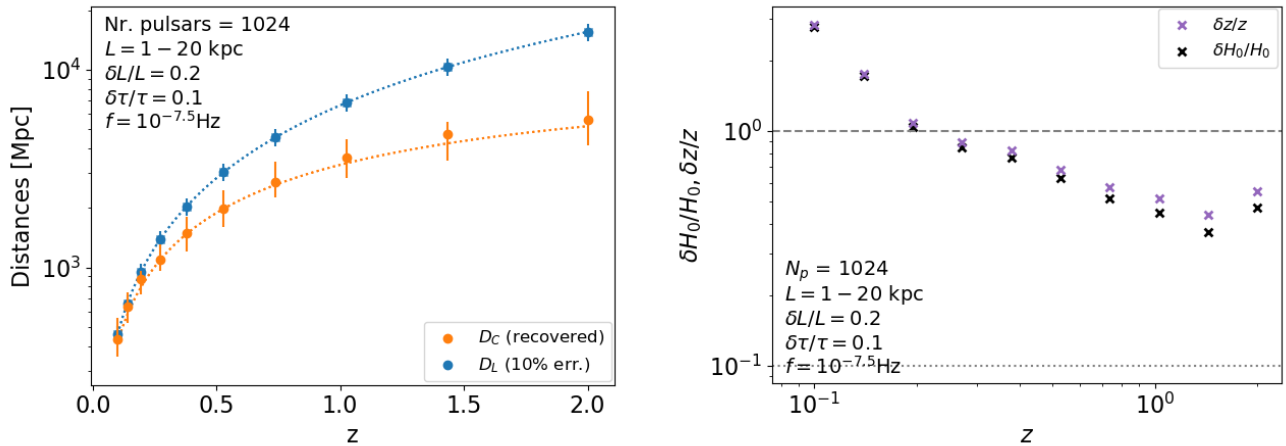


FIG. 4. Same as Figure 3, but for a scenario where many more pulsars can be timed but with less optimistic, 20% distance errors, and for a less optimal GW frequency of $10^{-7.5}$ Hz.

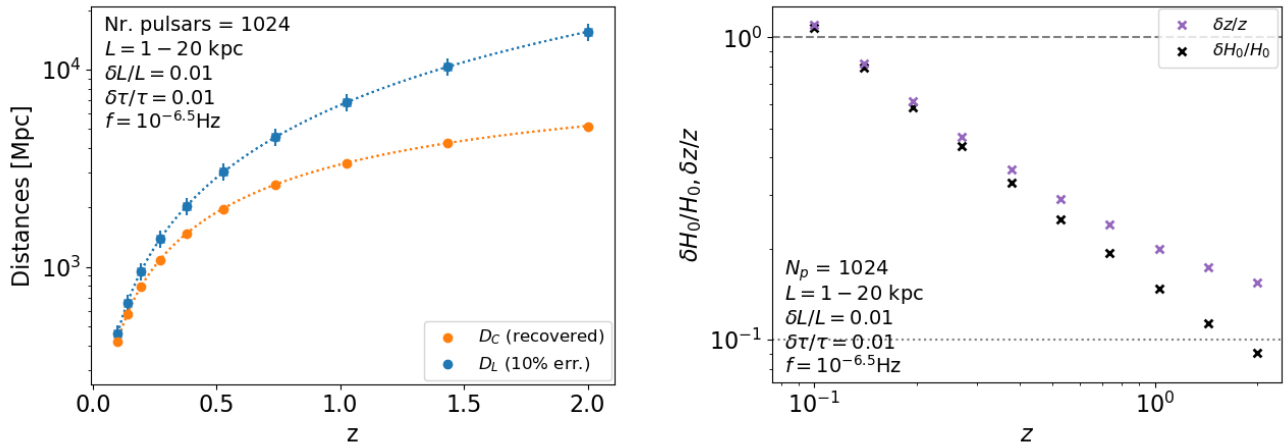


FIG. 5. Same as Figure 3, but for a best-case scenario with 1024 pulsars between 1 and 20 kpc with 1% distance and timing errors, and for a GW source with a high observed frequency $f = 10^{-6.5}$ Hz.

sioned here, with 30 – 1000 pulsars between 1 and 20 kpc and with 1% – 10% distance errors, would be realized in the SKA era. Note that Ref. [38] considers only galactic pulsars (see their Fig. 1); pulsars in the Magellanic clouds could provide MSPs out to 40-60 kpcs [43–46]. In addition to the SKA, the next generation Very Large Array [ngVLA, 47] and astrometric pulsar distance measurements with WFIRST [48] will make the pulsar-distance fractional errors envisioned here even more feasible, making possible a 10% measurement of the Hubble constant from GWs alone. Such future arrays will also likely decrease the expected error in the luminosity distance measurement, and further reduce the error in the Hubble constant measurement described here.

If the Hubble constant can be measured in this manner for tens of sources, then a PTA-only measured value could reach better than 10% precision. While the number of such resolved ‘foreground’ binaries that will be detected is uncertain and relies on the poorly constrained SBHB population, multiple studies have attempted to estimate this number. Ref. [18] estimates that it may indeed be the resolved single binary sources that are detected before a stochastic GW background, with a detection every few years. Older models suggest that the number of such detections may be an order of magnitude lower [23–25]. Reassuringly, Ref. [23] shows that the most probable redshift range for resolved sources is between $0.2 \lesssim z \lesssim 1.5$, in the right range for the measurement envisioned here. However, [18] shows that while the resolved single sources are the most common at the higher GW frequencies considered here, in the $\sim 10^{-7.5} - 10^{-6.5}$ Hz range, their amplitudes are lower and the PTAs are less sensitive at these frequencies. This leads Ref. [18] to conclude that the optimal single-source *detection* frequencies for near future PTAs lie at $\sim 10^{-8}$ Hz. At these lower frequencies, the GW parallax measurement is much more difficult, requiring $\mathcal{O}(10)\times$ the number of pulsars to achieve the precision needed to differentiate luminosity and co-moving distances. Future work could analyze expected SBHB populations in light of the measurement at hand, quantifying how many sources per redshift and frequency will contribute to a meaningful measurement of the Hubble constant.

For nearby GW sources ($z \lesssim 0.1$), only upper bounds on the redshift and Hubble constant can be set because D_c and D_L are within 10% of each-other. This is partly due to our adopted 10% fractional error on the luminosity distance mea-

surement. If this can be improved upon, then one can take advantage of more nearby sources. In addition, because the co-moving distance can be measured to high precision for these nearby sources, its measurement could facilitate identification of the SBHB host galaxy (as discussed in DF11), and allow a standard-siren-type determination of the Hubble constant, as well as offer important astrophysical insight into, *e.g.*, the morphology of SBHB host galaxies.

While we have provided a proof-of-principle error estimation focusing on the largest error sources, future work should consider more realistic parameter estimation techniques, and the precision and accuracy to which all of the binary parameters can be recovered jointly [*e.g.*, 49, 50]. For example, by not modeling the orbital geometry of the GW source, we do not include binary inclination or GW polarization factors that would affect the degree with which inclination and luminosity distance can be disentangled. Finally, techniques that independently fit for the pulsar distances as part of the model [*e.g.*, 29] could enhance the precision of source parameter recovery presented here and should also be considered for application to cosmology with PTAs.

In summary, we have presented a novel method by which to measure the Hubble constant without the use of EM radiation, by assuming only general relativity, and without the need to model astrophysical properties of the emitting source of radiation. This measurement can be made uniquely by near future PTAs and could result in a single-source determination of the Hubble constant at the tens of percent level over the redshift range $z = 0.1 - 2$. Tens of such detections could yield a 10% measurement of the Hubble constant from gravitational signals from cosmological sources.

ACKNOWLEDGMENTS

We thank Stephen Taylor for helpful comments and Matthew C. Wilde for useful discussion during the preparation of this work. Financial support was provided through funding from the Institute for Theory and Computation Fellowship (DJD) and through the Black Hole Initiative which is funded by grants from the John Templeton Foundation and the Gordon and Betty Moore Foundation.

-
- [1] A. G. Riess, L. M. Macri, S. L. Hoffmann, D. Scolnic, S. Casertano, A. V. Filippenko, B. E. Tucker, M. J. Reid, D. O. Jones, J. M. Silverman, R. Chornock, P. Challis, W. Yuan, P. J. Brown, and R. J. Foley, *ApJ* **826**, 56 (2016), [arXiv:1604.01424](#).
 - [2] A. G. Riess, S. Casertano, W. Yuan, L. M. Macri, and D. Scolnic, *arXiv e-prints* (2019), [arXiv:1903.07603](#).
 - [3] Planck Collaboration, P. A. R. Ade, N. Aghanim, M. Arnaud, M. Ashdown, J. Aumont, C. Baccigalupi, A. J. Banday, R. B. Barreiro, J. G. Bartlett, and et al., *A&A* **594**, A13 (2016), [arXiv:1502.01589](#).
 - [4] H. S. Leavitt and E. C. Pickering, *Harvard College Observatory Circular* **173**, 1 (1912).
 - [5] B. F. Schutz, *Nature* (ISSN 0028-0836) **323**, 310 (1986).
 - [6] A. Krolak and B. F. Schutz, *General Relativity and Gravitation* **19**, 1163 (1987).
 - [7] D. E. Holz and S. A. Hughes, *The Astrophysical Journal* **629**, 15 (2005).
 - [8] C. Cutler and D. E. Holz, *Physical Review D* **80**, 104009 (2009).
 - [9] B. P. Abbott, R. Abbott, T. D. Abbott, F. Acernese, K. Ackley, C. Adams, T. Adams, P. Addesso, R. X. Adhikari, V. B. Adya,

- and et al., *Nature* **551**, 85 (2017), arXiv:1710.05835.
- [10] H.-Y. Chen, M. Fishbach, and D. E. Holz, *Nature* **562**, 545 (2018), arXiv:1712.06531.
- [11] M. Rigault, V. Brinnet, and G. e. a. Aldering, arXiv e-prints (2018), arXiv:1806.03849.
- [12] S. R. Taylor and J. R. Gair, *PRD* **86**, 023502 (2012), arXiv:1204.6739 [astro-ph.CO].
- [13] S. R. Taylor, J. R. Gair, and I. Mandel, *PRD* **85**, 023535 (2012), arXiv:1108.5161 [gr-qc].
- [14] B. P. Abbott and R. e. a. Abbott, *Reports on Progress in Physics* **72**, 076901 (2009), arXiv:0711.3041 [gr-qc].
- [15] P. Amaro-Seoane and et al., ArXiv e-prints (2017), arXiv:1702.00786 [astro-ph.IM].
- [16] X. Deng and L. S. Finn, *MNRAS* **414**, 50 (2011), arXiv:1008.0320 [astro-ph.CO].
- [17] A. N. Lommen, *Journal of Physics Conference Series* **363**, 012029 (2012).
- [18] L. Z. Kelley, L. Blecha, L. Hernquist, A. Sesana, and S. R. Taylor, *MNRAS* **477**, 964 (2018), arXiv:1711.00075 [astro-ph.HE].
- [19] J. P. W. Verbiest and G. M. Shaifullah, *Classical and Quantum Gravity* **35**, 133001 (2018).
- [20] S. Burke-Spolaor, S. R. Taylor, M. Charisi, T. Dolch, J. S. Hazboun, A. M. Holgado, L. Z. Kelley, T. J. W. Lazio, D. R. Madison, N. McMann, C. M. F. Mingarelli, A. Rasskazov, X. Siemens, J. J. Simon, and T. L. Smith, *A&A Review* **27**, 5 (2019), arXiv:1811.08826 [astro-ph.HE].
- [21] X. Siemens, J. Ellis, F. Jenet, and J. D. Romano, *Classical and Quantum Gravity* **30**, 224015 (2013), arXiv:1305.3196 [astro-ph.IM].
- [22] S. R. Taylor, M. Vallisneri, J. A. Ellis, C. M. F. Mingarelli, T. J. W. Lazio, and R. van Haasteren, *ApJL* **819**, L6 (2016), arXiv:1511.05564 [astro-ph.IM].
- [23] A. Sesana, A. Vecchio, and M. Volonteri, *MNRAS* **394**, 2255 (2009), arXiv:0809.3412 [astro-ph].
- [24] V. Ravi, J. S. B. Wyithe, R. M. Shannon, G. Hobbs, and R. N. Manchester, *MNRAS* **442**, 56 (2014), arXiv:1404.5183 [astro-ph.CO].
- [25] P. A. Rosado, A. Sesana, and J. Gair, *MNRAS* **451**, 2417 (2015), arXiv:1503.04803 [astro-ph.HE].
- [26] D. J. D’Orazio and A. Loeb, *PRD* **101**, 083031 (2020), arXiv:1910.02966 [astro-ph.HE].
- [27] A. Sesana and A. Vecchio, *PRD* **81**, 104008 (2010), arXiv:1003.0677 [astro-ph.CO].
- [28] N. J. Cornish, arXiv e-prints, gr-qc/0304020 (2003), arXiv:gr-qc/0304020 [gr-qc].
- [29] K. J. Lee, N. Wex, M. Kramer, B. W. Stappers, C. G. Bassa, G. H. Janssen, R. Karuppusamy, and R. Smits, *MNRAS* **414**, 3251 (2011), arXiv:1103.0115 [astro-ph.HE].
- [30] S. R. Taylor, E. A. Huerta, J. R. Gair, and S. T. McWilliams, *ApJ* **817**, 70 (2016), arXiv:1505.06208 [gr-qc].
- [31] V. Corbin and N. J. Cornish, arXiv e-prints, arXiv:1008.1782 (2010), arXiv:1008.1782 [astro-ph.HE].
- [32] R. Angéilil and P. Saha, *PRD* **91**, 124007 (2015), arXiv:1505.03157 [gr-qc].
- [33] L. S. Finn and A. N. Lommen, *ApJ* **718**, 1400 (2010), arXiv:1004.3499 [astro-ph.IM].
- [34] M. Anholm, S. Ballmer, J. D. E. Creighton, L. R. Price, and X. Siemens, *PRD* **79**, 084030 (2009), arXiv:0809.0701 [gr-qc].
- [35] L. G. Book and É. É. Flanagan, *PRD* **83**, 024024 (2011), arXiv:1009.4192 [astro-ph.CO].
- [36] D. Foreman-Mackey, D. W. Hogg, D. Lang, and J. Goodman, *PASP* **125**, 306 (2013), arXiv:1202.3665 [astro-ph.IM].
- [37] J. Goodman and J. Weare, *Communications in Applied Mathematics and Computational Science* **5**, 65 (2010).
- [38] R. Smits, S. J. Tingay, N. Wex, M. Kramer, and B. Stappers, *A&A* **528**, A108 (2011), arXiv:1101.5971 [astro-ph.IM].
- [39] F. Combes, *Journal of Instrumentation* **10**, C09001 (2015), arXiv:1504.00493 [astro-ph.CO].
- [40] G. Janssen, G. Hobbs, M. McLaughlin, C. Bassa, A. Deller, M. Kramer, K. Lee, C. Mingarelli, P. Rosado, S. Sanidas, A. Sesana, L. Shao, I. Stairs, B. Stappers, and J. P. W. Verbiest, in *Advancing Astrophysics with the Square Kilometre Array (AASKA14)* (2015) p. 37, arXiv:1501.00127 [astro-ph.IM].
- [41] C. M. F. Mingarelli, L. Anderson, M. Bedell, and D. N. Spergel, arXiv e-prints, arXiv:1812.06262 (2018), arXiv:1812.06262 [astro-ph.IM].
- [42] C. Mingarelli, P. Baker, S. Chen, J. Hazboun, K. Islo, N. Pol, J. Simon, D. Reardon, S. Taylor, S. Vigeland, and International Pulsar Timing Array, in *American Astronomical Society Meeting Abstracts*, American Astronomical Society Meeting Abstracts (2020) p. 433.04.
- [43] F. Crawford, V. M. Kaspi, R. N. Manchester, A. G. Lyne, F. Camilo, and N. D’Amico, *ApJ* **553**, 367 (2001), arXiv:astro-ph/0011346 [astro-ph].
- [44] R. N. Manchester, G. Fan, A. G. Lyne, V. M. Kaspi, and F. Crawford, *ApJ* **649**, 235 (2006), arXiv:astro-ph/0604421 [astro-ph].
- [45] J. P. Ridley, F. Crawford, D. R. Lorimer, S. R. Bailey, J. H. Madden, R. Anella, and J. Chennamangalam, *MNRAS* **433**, 138 (2013), arXiv:1304.6412 [astro-ph.GA].
- [46] N. Titus, S. Toonen, V. A. McBride, B. W. Stappers, D. A. H. Buckley, and L. Levin, *MNRAS* **494**, 500 (2020), arXiv:2003.01969 [astro-ph.SR].
- [47] S. Chatterjee, in *Science with a Next Generation Very Large Array*, Astronomical Society of the Pacific Conference Series, Vol. 517, edited by E. Murphy (2018) p. 751.
- [48] WFIRST Astrometry Working Group, R. E. Sanderson, A. Bellini, S. Casertano, J. R. Lu, P. Melchior, M. Liralato, D. Bennett, M. Shao, J. Rhodes, S. T. Sohn, S. Malhotra, S. Gaudi, S. M. Fall, E. Nelan, P. Guhathakurta, J. Anderson, and S. Ho, *Journal of Astronomical Telescopes, Instruments, and Systems* **5**, 044005 (2019), arXiv:1712.05420 [astro-ph.IM].
- [49] S. Taylor, J. Ellis, and J. Gair, *PRD* **90**, 104028 (2014), arXiv:1406.5224 [gr-qc].
- [50] X. J. Zhu, L. Wen, G. Hobbs, Y. Zhang, Y. Wang, D. R. Madison, R. N. Manchester, M. Kerr, P. A. Rosado, and J. B. Wang, *MNRAS* **449**, 1650 (2015), arXiv:1502.06001 [astro-ph.IM].